ADVANCED FUNCTIONAL MATERIALS
www.afm-journal.de

A Thermodynamic Cycle-Based Electrochemical Windows Database of 308 Electrolyte Solvents for Rechargeable Batteries

*Da Wang, Tingting He, Aiping Wang, Kai Guo, Maxim Avdeev, Chuying Ouyang, Liquan Chen, and Siqi Shi**

Rational design of wide electrochemical window (ECW) electrolytes to pair with high-voltage cathodes is an emerging trend to push the energy density limits of current rechargeable batteries. Traditional single-electronic/gas-phase approximation-based methods (e.g., highest occupied molecular orbital/lowest unoccupied molecular orbital) are increasingly recognized to have large deviations from experiments when predicting ECWs of electrolytes involving complex solvent interactions. Specifically, by examining available experimental ECWs of 68 electrolyte solvents extracted from ≈140 000 literature sources, which are conventionally divided into five functional-group categories (covering commonly used carbonate-based ethylene carbonate (EC)/propylene carbonate (PC) and ether-based tetrahydrofuran), it is found that mean-absolute-errors (MAE) of traditional methods reach up to 3.25 V. Herein, a thermodynamic cycle-based ECW prediction approach is proposed including two long-term overlooked reorganization-energy and solvation-energy corrections, each of which can be quantified by two geometric descriptors (λ and ΔG_{sol}), reducing MAE below 0.68 V. Following this, a database containing ECWs for 308 electrolyte solvents, obtained by traversing single functional-group substitutions, is established. Furthermore, two omitted solvents with ECWs over 6.00 V and excellent structural stabilities (bond-length change < 0.10 Å during redox process) are retrieved by stepwise screening of structural/electronic parallel properties. This study demonstrates the benefits of improving ECW prediction accuracy and accumulating descriptors to accelerate rapid screening of superior battery electrolytes.

1. Introduction

With the increasing demand for energy worldwide for next-generation technologies such as electric vehicles, there is an urgent need to explore rechargeable batteries with high voltage and corresponding high energy density.[1] One of the key components in such batteries is electrolyte, which should exhibit as wide electrochemical window (ECW) as possible to match the rapidly developed high-voltage cathodes and thus push the limits of the energy density.[2] However, the currently adopted ECW prediction methods suffer from oversimplification of complex redox reaction as well as overemphasis on prediction convenience and efficiency, leading to growing controversy[3] and ultimately the inability of the commonly used organic compound databases, such as PubChem[4] and ChemSpider,[5] to provide accurate and comprehensive ECW information. Therefore, it is important to find a convenient and rapid approach to accurately predict the ECWs to facilitate the development of an ECW database for potential electrolytes for rechargeable batteries.[6]

D. Wang, T. He, K. Guo, S. Shi
School of Materials Science and Engineering
Shanghai University
Shanghai 200444, China
E-mail: sqshi@shu.edu.cn

D. Wang, S. Shi
Zhejiang Laboratory
Hangzhou, Zhejiang 311100, China

A. Wang
Institute of Nuclear and New Energy Technology
Tsinghua University
Beijing 100084, China

The ORCID identification number(s) for the author(s) of this article can be found under https://doi.org/10.1002/adfm.202212342.

M. Avdeev
Australian Nuclear Science and Technology Organisation
Locked Bag 2001, Kirrawee DC NSW 2232, Australia

C. Ouyang
Fujian Science & Technology Innovation Laboratory for Energy Devices of China (21C-LAB)
Ningde 352100, China

L. Chen
Institute of Physics
Chinese Academy of Sciences
Beijing 100190, China

S. Shi
Materials Genome Institute
Shanghai University
Shanghai 200444, China

DOI: 10.1002/adfm.202212342

Theoretically, multiple factors, such as complex redox reactions with different molecules or salts, concentrations, electrode materials, electrode surface states, temperatures, etc,[7] should be considered to achieve accurate predictions of the ECWs of electrolytes. The thermodynamic representation for the electrochemical stability based on redox potentials and Fermi level of the electron in solution $\left(E^{s}_{F,ox/red}\right)$ are usually written as:[3a]

$$E^{s}_{F,ox/red} = -e\left(\left[E^{\theta}_{ox/red}\right]^{S}_{SHE} + \frac{k_B T}{ne}\ln\left(\frac{\alpha^{S}_{ox}}{\alpha^{S}_{red}}\right) + \phi^{S} + \left[E^{\theta}_{H^+/\frac{1}{2}H_2}\right]_{AVS}\right) \quad (1)$$

where k_B and $\left[E^{\theta}_{H^+/\frac{1}{2}H_2}\right]_{AVS}$ are Boltzmann constant and the standard hydrogen electrode potential (4.44 V), respectively. T and α are temperature and activity in the standard state (298 K, 1 mol L^{-1}), respectively; $\phi^S = \chi^S$ (surface potential) + φ^S (outer potential) is the Galvani potential of the solution phase, which is rather complicated to take into account in the calculation.[3a,8] Based on this equation, the current common strategies for predicting ECW of electrolyte are essentially based on the standard hydrogen electrode potential $\left([E^{\theta}_{ox/red}]^{S}_{SHE}\right)$ regulation. Among them, the most widely used and simplest strategy is to use the energy level difference of the lowest unoccupied molecular orbital (LUMO) and the highest occupied molecular orbital (HOMO) to represent the electrolyte ECWs.[9] However, a growing number of studies have reported the inaccuracy of this method in predicting ECWs of electrolytes.[10] This is unsurprising, as traditional HOMO/LUMO derived from approximate electronic structure theory[11] represent electronic properties of isolated neutral molecules, from which the real ECWs of species' participation in redox reaction cannot be accurately predicted.[3a] For this reason, Peljo et al.[3a] even stated in a recent study that the use of terms HOMO/LUMO should be avoided when discussing ECWs of electrolytes.

Returning again to Equation 1, for the prediction ECW to be accurate they should consider that real redox reactions necessarily involve electron transfer. On this basis, the typical ionization potential (IP)/electron affinity potential (EA) method obtained from Koopmans' theorem is proposed as an improved approach to predicting ECW, which additionally considers charged molecules after electron transfer to solve the limitation of the HOMO/LUMO method that only considers neutral molecules. The IP/EA method has been already used in the field of rechargeable batteries.[12] For example, Persson et al.[12c] emphasize that IP/EA method is more stringent than the often-applied HOMO/LUMO method during the screening of ECWs for new magnesium electrolytes. Unfortunately, the IP/EA method is still found to be surprisingly inaccurate in predicting electrolyte ECWs with complex local environments when compared to the experimental values.[13] A critical question remains though: how to develop a rapid and accurate method by taking into account complex local environments for screening electrolytes with wide ECWs?

In this work, by examining available experimental oxidation potentials of 68 electrolyte solvents, which are conventionally divided into five functional-group categories (viz., Amide, Nitrile, Ether, Carbonate, and Sulfone), we find that mean-absolute-errors (MAE) of traditional methods (e.g., HOMO/LUMO) reach up to 3.25 V, validating the irrationality of these methods in predicting the ECWs of electrolytes. Following this, a thermodynamic cycle approach including the reorganization-energy and solvation-energy corrections is proposed, controlling the ECW prediction MAE of above 68 experimentally reported solvents to be within 0.68 V. On this basis, a database containing thermodynamic cycle ECWs, structure parameters, and physicochemical properties of 308 solvents is established. Finally, by stepwise screening of the structural/electronic properties and comparing the experimental data, a retrieval of two omitted solvents with wide ECWs and excellent structural stabilities is achieved.

2. Calculation Details and Methodology

2.1. Calculation Details

All calculations in this article are performed using Gaussian 09.[14] Geometry optimizations are carried out at the B3LYP[15]/6-311+G(d)[16] level and frequency calculations are performed at the same theoretical level. This is because considering the practical computational cost and accuracy for >300 electrolyte solvents, the B3LYP/6-311+G(d) is explored to be the functional with most reliable average performance, and can show good consistency with high-precision single-point energy calculations, as shown in Figure S1 (Supporting Information). Specifically, frequency calculations confirm that each final optimized geometric configuration has a minimum value on the potential energy surface without any imaginary frequency. The single-point energy calculation is followed at the B3LYP/6-311+G(d) level. Considering that the energy of electron transfer process in electrochemical reactions (whether a single-electron or a multi-electron transfer reaction occurs[17]) of a majority of organic systems used in battery electrolytes is always dominated by the first electron transfer energy, only single-electron transfer is considered.

2.2. Calculation Methodology

For ECW obtained from the energy of highest occupied molecular orbital (HOMO) and lowest unoccupied molecular orbital (LUMO), $V = \frac{LUMO}{e} - \frac{HOMO}{e}$, where e is the electron charge. Besides, the ECW calculated by the ionization potential (IP) and the electron affinities (EA) can be written as $V = \frac{IP}{e} - \frac{EA}{e}$, where IP = E_g ($N-1$) − E_g(N), EA = E_g (N) − E_g($N+1$). E_g(N), E_g($N+1$) and E_g($N-1$) are the gas energy of neutral molecules, corresponding anions and cations, and N is the number of electrons in the original molecule, respectively.

We propose a thermodynamic cycle approach that takes into account the solvent effect and geometric relaxation to calculate the single-electron redox potentials of solvents. According to the thermodynamic cycle shown in **Figure 1**, $\Delta G^{ox}_{sol}(A)$ and $\Delta G^{red}_{sol}(A)$ can be calculated from the Gibbs free energy change:

$$\Delta G^{red}_{sol}(A) = -\Delta G_{sol}(A) + \Delta G^{red}_{g}(A) + \Delta G_{sol}\left(A^-\right) + \Delta n \Delta G^{\circ\rightarrow *} \quad (2)$$

$$\Delta G^{ox}_{sol}(A) = -\Delta G_{sol}(A) + \Delta G^{ox}_{g}(A) + \Delta G_{sol}\left(A^+\right) + \Delta n \Delta G^{\circ\rightarrow *} \quad (3)$$

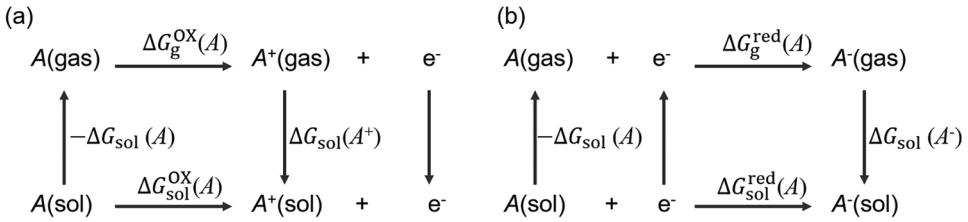

Figure 1. Thermodynamic cycles for the redox reaction. a) Oxidation process. b) Reduction process. Species in the gas phase and in solution are indicated by "(g)" and "(sol)", respectively.

$$\Delta G_g^{ox}(A) = G_g(A^+) - G_g(A),\ \Delta G_g^{red}(A) = G_g(A^-) - G_g(A) \quad (4)$$

where $\Delta G_g^{ox}(A)$ and $\Delta G_g^{red}(A)$ are the free energy of oxidation and reduction of neutral solvent molecule A in the gas phase. $\Delta G_{sol}^{ox}(A)$ and $\Delta G_{sol}^{red}(A)$ are the Gibbs free energy change of oxidation and reduction of neutral solvent molecule A in the solution phase, respectively. Solvation energy is the energy required to transfer molecules or ions from vacuum to solution phase, $\Delta G^{\circ\to *}$ is the correction factor for converting the standard state of a substance from 1 atm to 1 mol L^{-1}, and Δn is the change in the number of moles.[18] Since the energy change of electrons from vacuum to the non-aqueous solution is small, the solvation energy of electrons is neglected.[19]

To compare with experimental data, the calculated value must be converted to relative potential. Here a value of 1.44 V[20] is adopted to convert the absolute scale to Li^+/Li, ignoring the difference between solvents expected to be about a few tenths of a volt.[21] Thus, redox potentials of organic solvent molecules relative to the Li metal (vs. Li^+/Li) can be calculated from the above $\Delta G_{sol}^{ox}(A)$ and $\Delta G_{sol}^{red}(A)$:

$$E_{ox} = \frac{\Delta G_{sol}^{ox}(A)}{n\mathrm{F}} - 1.44 \quad (5)$$

$$E_{red} = -\frac{\Delta G_{sol}^{red}(A)}{n\mathrm{F}} - 1.44 \quad (6)$$

where F is Faraday constant, n is the electron number participating in the redox reaction.

The mean absolute error (MAE) is calculated to evaluate the accuracy of the different methods for predicting the oxidation/reduction potentials of organic solvents:

$$\mathrm{MAE} = \frac{\sum |\mathrm{Allcomputational} - \mathrm{Allexperimental}|}{\mathrm{N}} \quad (7)$$

where *Allcomputational* and *Allexperimental* indicate the calculated and experimentally measured redox potentials, respectively; N is organic solvent number.

3. Results and Discussion

3.1. Identification of Two Factors Contributing to Large MAE of Traditional Methods

We first theoretically clarify the accuracy of traditional HOMO/LUMO method in predicting experimental redox potentials. Considering that the main challenge of designing a wide ECW electrolyte is to broaden its oxidation potential, we focus only on evaluating the difference between the calculated HOMO values and the real oxidation potentials. To achieve this goal, 68 electrolyte solvents with experimentally reported ECW values and no irreversible structural changes in the redox reaction are screened from 141427 theoretical/experimental research papers on rechargeable batteries (including Li-ion and post-Li-ion batteries) published in the past decade (Figure S2, Supporting Information). These solvents including the commonly used EC/PC and tetrahydrofuran can be divided into five categories as in our previous work,[22] viz., Amide, Nitrile, Ether, Carbonate, and Sulfone, whose detailed codes, experimental reduction potentials and other physicochemical properties are summarized in Tables S1–S3 (Supporting Information). At the same time, we emphasize that the intrinsic ECW (oxidation and reduction potential) is calculated for isolated electrolyte component, without consideration of salt/additive/co-solvent and electrode surface effect.[13a]

It can be seen from **Figure 2**a and Table S1 (Supporting Information)that for all 68 solvents the calculated HOMO values are overestimated compared with the experimentally measured oxidation potentials. Among them, small deviations (<0.35 V vs. absolute vacuum scale), especially for some simple solvents with molecular weights <90 g mol^{-1} can be observed. For example, the HOMO values of the commonly used Ethylene carbonate (EC) and Dimethyl carbonate (DMC) solvents, are calculated to be –8.47 and –8.21 eV, which are in good agreement with the experimental predictions of 8.14[23] and 8.14 V[24] versus absolute vacuum scale. This explains the widespread use of the HOMO/LUMO method in predicting ECWs.

Overall, however, the MAE between the HOMO values and the experimental oxidation potentials reaches 1.03 V (vs. absolute vacuum scale). It is therefore evident that the ECWs of solvents estimated by HOMO/LUMO calculation are generally large, that is, they can only give the upper limit of ECWs of systems. More importantly, it is precisely because the upper limit of these excess prediction has reached a maximum of 46%, leading to a great controversy over the validity of the prediction of HOMO/LUMO method.[3a] We emphasize that the essence of the above controversy stems from the fact that the HOMO/LUMO method is based on approximate electron structure theory, which fixes the molecular structures and only considers their neutral state, thereby ignoring the electron transfer between reactants (neutral molecules) and products (charged molecules) as well as the structural evolution in the redox reaction.

The accuracy of predicting the ECW of systems is expected to be improved in the IP/EA method, which considers the electron transfer in the redox reaction, thus correcting the error caused by the extreme simplification neutral condition in the HOMO/LUMO method. It is well known that the linear

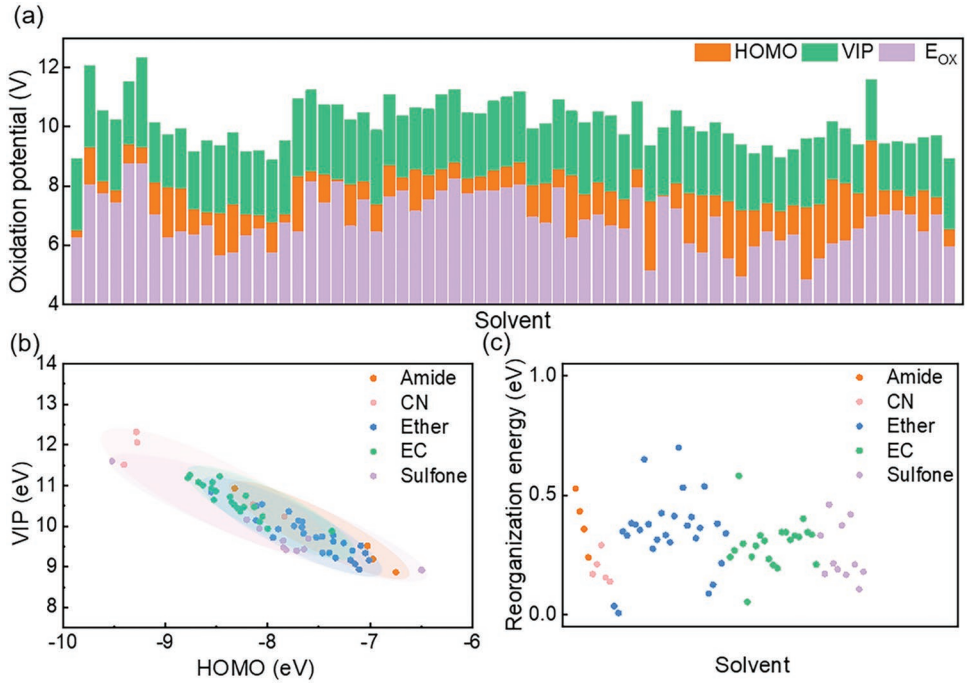

Figure 2. a) Calculated oxidation potentials of 68 solvents by HOMO method (in V vs. absolute vacuum scale), and VIP method (in V vs. absolute vacuum scale) compared to the experimental values (E_{OX} in V, vs. absolute vacuum scale). The detail information of 68 solvents divided into five categories (Amide, Nitrile, Ether, Carbonate and Sulfone) can be obtained from the remarks at the bottom of Table S1 (Supporting Information). Details of the conversion of potentials between the above methods are described in the Section on Calculation methodology. b) Correlation between HOMO and VIP for 68 solvents. c) Distribution of reorganization energy (in eV) related to VIP and AIP for 68 solvents.

relationship between vertical ionization potential (VIP)/vertical electron affinity (VEA) and HOMO/LUMO can be obtained directly according to the Koopmans' approximation theorem.[25] This is well confirmed in the linear correlation between VIP and HOMO values of the above mentioned 68 solvents (with the negative correlation coefficient of 0.84, Figure 2b). However, it is especially noteworthy that the VIP values not only overestimate the experimental oxidation potentials, but have even larger MAE (up to 3.25 V vs. absolute vacuum scale) than the HOMO values, as can be seen in Figure 2a and Table S1 (Supporting Information). We first exclude the inaccuracy of VIP/VEA method to clarify its overestimation of experimental potentials compared to the HOMO/LUMO method. We compare available experimental VIP values of 24 solvents from the National Institute of Standards and Technology database with calculated VIP values, as shown in Figure S3 and Table S4 (Supporting Information). It is seen that the DFT-derived VIP values agree well with the experimental values with a MAE of 0.27 eV. This shows the accuracy of our calculation method, and verifies the overestimation of VIP/VEA method in predicting oxidation potentials of solvents. The underlying reason for this phenomenon is that although because that although the Koopmans' approximation emphasizes the importance of describing real non-neutral redox environment, it ignores the electronic correlation and classical Coulomb electrostatic energy during the redox reaction process. That is, when an electron is transferred, the charges on remaining orbitals undergo spatial rearrangement, resulting in derivative discontinuity (Δ_{XC} = constant > 0) associated with electronic correlation and identical shifts $\left(\frac{e^2}{C}\right)$ associated with Coulomb electrostatic energy, where C is the capacitance of the molecular system and e is the elementary charge.[26] This also explains the deviation of up to several electron volts between calculated HOMO energy and experimental ionization energy. In addition, it is found that the range of oxidation potential values predicted by HOMO/LUMO method or VIP/VEA method is not consistent regardless of the solvent category of the molecule. This suggests that the essential reason affecting the magnitude of potentials is not the solvent category, but may be due to the properties of its substituted functional groups. Even so, the above linear relationship clearly shows that that although the VIP/VEA method still cannot accurately predict the ECW, it provides a necessary condition of reaction non-neutrality and possible further improvement of the prediction accuracy of the theoretical model.

On this basis, we further investigate the effectiveness of the AIP method, which takes into account electron and nucleus reconstruction by optimizing the geometry of neutral and charged molecules, in predicting the ECW of solvent systems. Figure S4 (Supporting Information) shows the energy difference ($\Delta E_{VIP-AIP}$) between VIP and AIP for 68 solvents. Interestingly, it is noted that $\Delta E_{VIP-AIP}$ are always larger than 0. This is reasonable because after the transfer of electrons, the relaxation of the positively charged structure results in the decrease of the system energy to form a relatively stable structure (Figure S5, Supporting Information).[27] Thus, we define $\Delta E_{VIP-AIP}$ caused by the above-mentioned geometrical relaxation (reorganization) as the reorganization energy descriptor (λ) during the oxidation process.[28] It can be seen from Figure 2c that the reorganization

energy of all 68 solvents varies from 0 to 0.58 eV, further emphasizing the key role of reorganization energy in the redox reaction process.

We next explore the key factors that determine the above reorganization energy. It is observed that the range of reorganization energy varies regardless of the solvent category of the molecule. That is because the fundamental reason affecting the magnitude of reorganization energy is not the solvent category, but the changes of geometric properties (bond length, bond angle and dihedral angle changes) caused by structural relaxation between the neutral and the cationic states.[29] Thus, we first investigate the relationship between these three geometric properties and reorganization energy. As shown in **Figure 3**a, there is no significant linear correlation between any geometric property and reorganization energy, indicating that reorganization energy cannot be determined uniquely by a single geometric factor. This is also confirmed by Hutchison et al.,[30] who proposed in the study of organic oligoheterocycles that the reorganization energy is related to the function of a linear combination of the changes in bond length (ΔL) and dihedral angle (ΔD) on oxidation from the neutral to the corresponding cation.

Based on this, we examine the geometric distortion caused by charge transfer in 68 solvents, and propose a geometric descriptor that quantitatively describes relationship between ΔL and coupled ΔD factor:

$$\lambda = C_0 + C_1\Delta L + C_2\Delta D \quad (8)$$

where C_0, C_1, and C_2 are the coefficients from the multivariate least-squares fit, which are determined to be 0.08, 6.97, and 0.004 in our work, respectively. According to this descriptor, we find that the MAE between calculated reorganization energy and predictive reorganization energy is 0.08 eV and the analysis of variance value F[31] is 15.85 (Figure 3b) for 68 solvents, where calculated MAE is 4%–38% lower than considering single geometric factor, for either solvent category. This not only demonstrates that using this descriptor can improve accuracy, but also further proves that a single geometric factor or solvent category cannot determine the reorganization energy. Furthermore, the coefficients in λ are all larger than 0, further confirming that the reorganization energy is always higher than 0. Thus, the oxidation potentials predicted by the AIP method are compared with the measured experimentally, as presented in Figure 3c and Table S1 (Supporting Information). The results show that compared with VIP method, AIP method could improve the accuracy of oxidation potential prediction with an MAE of 2.99 V (vs. absolute vacuum scale), which also confirms the validity of reorganization energy correction. Most importantly, it can be also seen in Figure 3c that there is still a significant difference between the AIP predicted value and the experimental value, indicating that the prediction accuracy of this method is still insufficient even if the reorganization energy is considered by our proposed geometric descriptor (λ). Therefore, a method considering the influence of more complex local environment and other factors needs to be urgently proposed.

3.2. Proposing a Thermodynamic Cycle Approach Including Solvent Effects and Geometric Relaxation Corrections

In view of the inaccuracies of the above-mentioned traditional methods in predicting ECWs of common solvents, here we

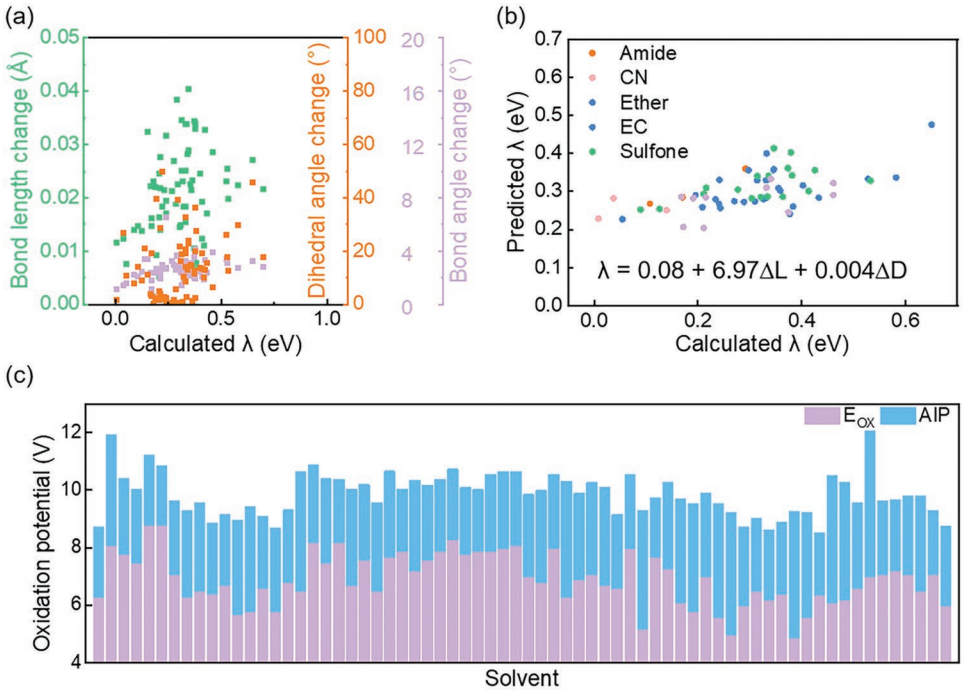

Figure 3. Correlation between the calculated reorganization energies (λ) of 68 organic solvents and a) average bond length, bond angle and dihedral angle changes between their neutral and cationic states, and b) the predicted reorganization energy. The established linear equation for λ and bond length (ΔL)/dihedral angle factors (ΔD) is also listed. c) comparation of oxidation potentials of 68 organic solvents calculated by AIP method (in eV) with experimental values (E_{OX} in V, vs. absolute vacuum scale). Details of the conversion of potentials between the above methods are described in the Section on Calculation methodology.

propose a high-accuracy thermodynamic cycle-based ECW prediction approach that corrects for bulk solvent effects (which are neglected in the above AIP method[32]) by implicit solvent model and geometric relaxation (neglected by both VIP and HOMO methods) by reorganization energy (Figure S6, Supporting Information). First, considering the complexity of molecular interactions and the diversity of solvents related to polarity in organic solvents for rechargeable batteries, we test the accuracy of three different implicit solvation models,[33] viz., polarizable continuum model (PCM), conductor-like screening model (COSMO), and solvation model density (SMD), for predicting their bulk solvent effects (Figure S7, Supporting Information). The results show that the oxidation potentials of the above 68 solvents calculated by using the SMD model to describe the solvent energy of systems are in good agreement with the experimental values (with the calculated MAE lower than 0.68 V vs. Li^+/Li). For example, Lim et al.[34] found that 3 M_{solv} LiFSI 1,2-Dimethoxy ethane (DME): Furan-(1: 2) electrolyte can exhibit high oxidation potential (≈4.50 V vs. Li^+/Li) by linear sweep voltammetry (LSV), which is in good agreement with our calculated intrinsic values using the SMD model (DME: 4.90 V vs. Li^+/Li, Furan: 4.73 V vs. Li^+/Li). Martins et al.[35] also reported previously that SMD method can provide more accurate solvation free energy calculation results (with a lowest average mean unsigned error) compared with PCM and COSMO methods for specific alcohol-based molecule systems.

As we further analyze the essential reason for the more accurate prediction of SMD model, it is found that for the uncharged solvents without any polar functional groups, their non-electrostatic effects are likely to be much larger than the electrostatic effects,[36] e.g., the non-electrostatic energy of DME reaches 1.05 kcal mol^{-1}. In this regard, the SMD model can produce more accurate results because not only it considers the electrostatic solute–solvent interaction of the PCM model,[37] but also contains the non-electrostatic interactions (cavity-dispersion-solvent-structural term[33]). Notably, the SMD non-electrostatic terms do not alter the electron density from the PCM model but will change the electron density and the resulting excitation energy due to the different atomic radii used to define the van der Waals surface.[38] This may account for the different numerical results of PCM (radii = United Atom Hartree-Fock and SMD (radii = SMD-CoulOMb) models. Because of this, for the solvents commonly used in the field of electric energy storage, the PCM model can only provide a rough estimate of the variation in electron distribution.[39] In conclusion, we determine that SMD with non-electrostatic interaction is more suitable for organic solvents used in battery. Therefore, the subsequent calculated redox potentials are all derived from the thermodynamic cycle approach based on the SMD solvation model.

Subsequently, we analyze the factors that determine the solvation energy obtained with the SMD model. When we compared the AIP values of 68 solvents, which ignored the solvent effect, with their absolute oxidation potentials, it is found that the energy differences range widely from 1.71 to 3.01 eV (**Figure 4**a). For example, the AIP of EC is calculated to be 10.88 eV, while its measured oxidation potential is only 6.90 V versus Li^+/Li. Crucially, there is a strong linear correlation between the above energy differences and the solvation energy (Figure S8, Supporting Information), further highlighting the importance of solvation energy in the oxidation process of single-electron transfer. Here, the solvation energy can be represented by the energy change of a molecule from the neutral to the cationic state in the solution phase as defined by: $\Delta G_{sol} = \Delta G_{sol}(A^+) - \Delta G_{sol}(A)$, where $\Delta G_{sol}(A^+)$ and $\Delta G_{sol}(A)$ denote the solvation free energies of the cationic and neutral states, respectively,[40] which have been proved to be related to the polarity of the solute/solvent molecular interaction force[41] and molecular size[42] rather than solvent category. However, we verify that there was no significant correlation between the polarity (that can be represented by the solvent dipole moment) and the solvation energies of solvent molecular systems, as shown in Figure 4b. For example, the dipole moment of Acetonitrile (ACN) is almost the same as that of Triethyl phosphate (≈3.99 Debye), but their solvation energies are calculated to be −2.94 and −1.70 eV, respectively, which are greatly different (Table S1, Supporting Information). Notably, when we further study the relationship between molecular volume (V_{mol}) and solvation energy, a significant positive correlation can be observed between them, viz., solvents with larger molecular volumes tend to exhibit greater solvation energies (Figure 4c). For example, molecular volumes of *N*-methylacetamide (NMA)/Dimethyl acetamide (amide-based category) and dioxolane/DME (ether-based category) are 108.72/131.21 and 97.33/137.75 $Å^3$, where their solvation energies are −2.60/−2.54 and −2.67/−2.42 eV, respectively. This confirms that the magnitude of the solvation energy is indeed influenced by the molecular size.

Based on the above two defined geometric descriptors (λ and ΔG_{sol}), we achieve the quantitative prediction of reorganization energy and solvation energy, which are two factors affecting the accuracy of theoretical methods to calculate ECW. Finally, we compare the ECWs of 5 common solvents calculated by the proposed thermodynamic cycle approach, which includes the consideration of bulk solvent effect by SMD model and reorganization energy due to structural relaxation during single-electron transfer, with those measured experimentally (**Figure 5**a). It is observed that compared with the unacceptable MAE of traditional HOMO/LUMO, VEA/VIP, and AEA/AIP methods in predicting the ECW, which are 2.00, 5.67, and 5.40 V versus Li^+/Li, the accuracy of the proposed approach is significantly improved with the MAE of only 0.36 V.

All in all, we verify the intrinsic limitations of traditional HOMO/LUMO and VIP/VEA (or AIP/AEA) methods in predicting ECWs of electrolytes, and summarize a complete picture of origins of their respective errors in Figure 5b. It is precisely because the HOMO/LUMO is based on the simplest neutral approximation of the electronic structural framework that results in its inability to accurately predict redox potentials of solvents (with MAE > 1.03 V versus absolute vacuum scale in this work, yellow ball in Figure 5b). Therefore, the introduction of VIP/VEA method involving Koopmans' approximation to account for charge transfer effect breaks the above constraint of predicting ECWs under neutral condition. However, in real redox reactions, the organic solvent ionic structure after electron transfer leads to a decrease in system energy by electron/nucleus reorganization, that is, reorganization energy. Due to the lack of this energy correction, VIP/VEA method only

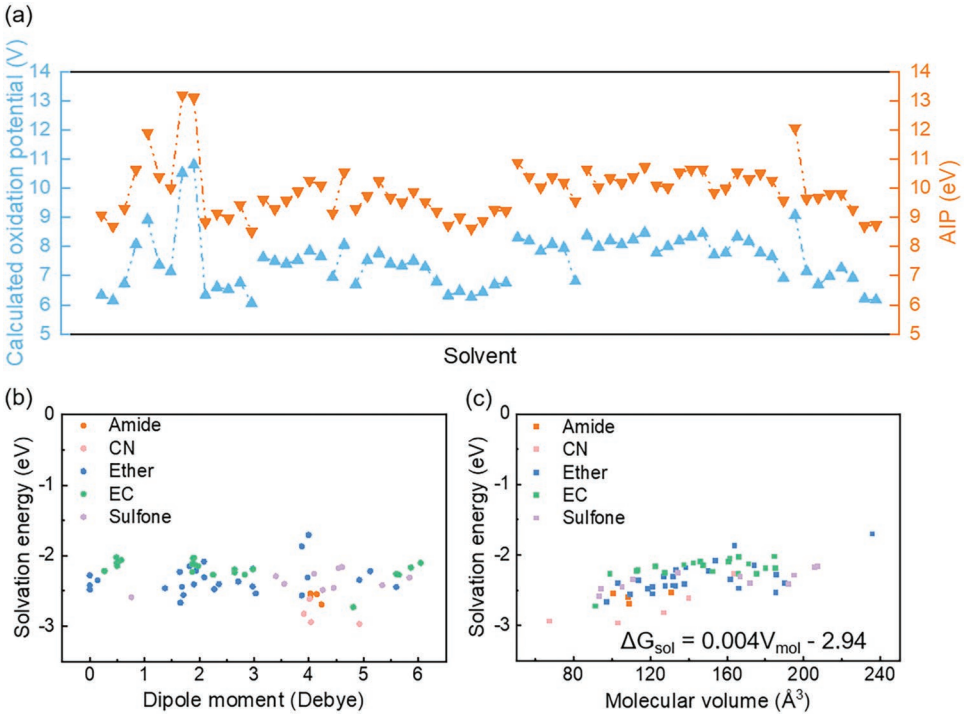

Figure 4. a) Correlation between AIP values (in eV) and oxidation potentials calculated by thermodynamic cycle approach (in V, vs. absolute vacuum scale) for 68 organic solvents. Details of the conversion of potentials between above methods are described in Calculation methodology. Yellow and blue lines represent AIP and calculated oxidation potentials, respectively. Correlation between solvation energy (ΔG_{sol}) and b) dipole moment or c) molecular volume for 68 solvents.

makes prediction in fixed molecular cases still deviate significantly from experimental ECWs (with MAE > 3.25 V vs. absolute vacuum scale in this work, green ball in Figure 5b). We thus further improve the ECW prediction accuracy by using AIP/AEA method, that can simultaneously optimize the neutral and charged molecule geometries, and propose a key reorganization-energy correction (λ, Equation 8). The reduction of prediction MAE (2.99 V vs. absolute vacuum scale in this work, blue ball in Figure 5b) also confirms the necessity of considering structural reorganization during redox reaction. Finally, considering that the real redox reactions are carried out in solvent phase, we also propose a solvation energy descriptor (ΔG_{sol}) and uncover its quantitative linear correlation with the molecular size (V_{mol}, Figure 4c). On this basis, a high-accuracy thermodynamic cycle-based intrinsic ECW prediction approach that comprehensively considered the above correction is proposed, which successfully reduces the MAE to < 0.68 V versus Li^+/Li (purple ball in Figure 5b, viz., with a 34.31% decrease in MAE compared to above HOMO/LUMO method, Figure S9, Supporting Information), enabling accurate computational screening for promising electrolytes. Furthermore, for any category of solvents, the error between oxidation potentials calculated by the proposed thermodynamic cycle approach and experimental values can be reduced compared to the traditional HOMO/LUMO method, as shown in the Table S5 (Supporting Information). This again suggests that, regardless of the solvent category, long-term overlooked reorganization-energy and solvation-energy corrections can be identified as the keys to the inaccuracy of ECWs predicted by traditional methods.

Moreover, it is worth noting that the prediction accuracy improvement of ECWs mainly depends on the description of the oxidation process. Taking the ECW modification of DMC as an example, its ECW calculated by the HOMO/LUMO method is 8.29 V versus absolute vacuum scale and the corrected ECW by thermodynamic cycle approach is 6.95 V versus Li^+/Li, where the reorganization energy and the solvation energy of the oxidation (reduction) process are calculated to be 0.38 (0.01), −2.21 (−2.25) eV, respectively. It can be seen that these two energetic corrections in the reduction process is smaller than that in the oxidation process. Therefore, the correction for the reduction potential can be neglected compared to that for the oxidation potential. In addition, based on a basic understanding of different calculated HOMO/LUMO mean, it is found that all HOMO energies and experimental oxidation potentials have a large gap, as shown in Figure S10 (Supporting Information). This indicates that, HOMO/LUMO method, even considering local environmental and geometric relaxation, is difficult to achieve good agreement with the experiment. Therefore, it is necessary to introduce the VIP/VEA method involving Koopmans' approximation to account for charge transfer effect for breaking the above constraint of predicting ECWs under neutral condition.

A complete picture from the traditional HOMO/LUMO method, which is unable to predict ECWs of electrolytes (including five most typical functional-groups, upper right inset and represented here by placing stones to block the gray road), to the proposed high-accuracy thermodynamic cycle approach that comprehensively considered reorganization

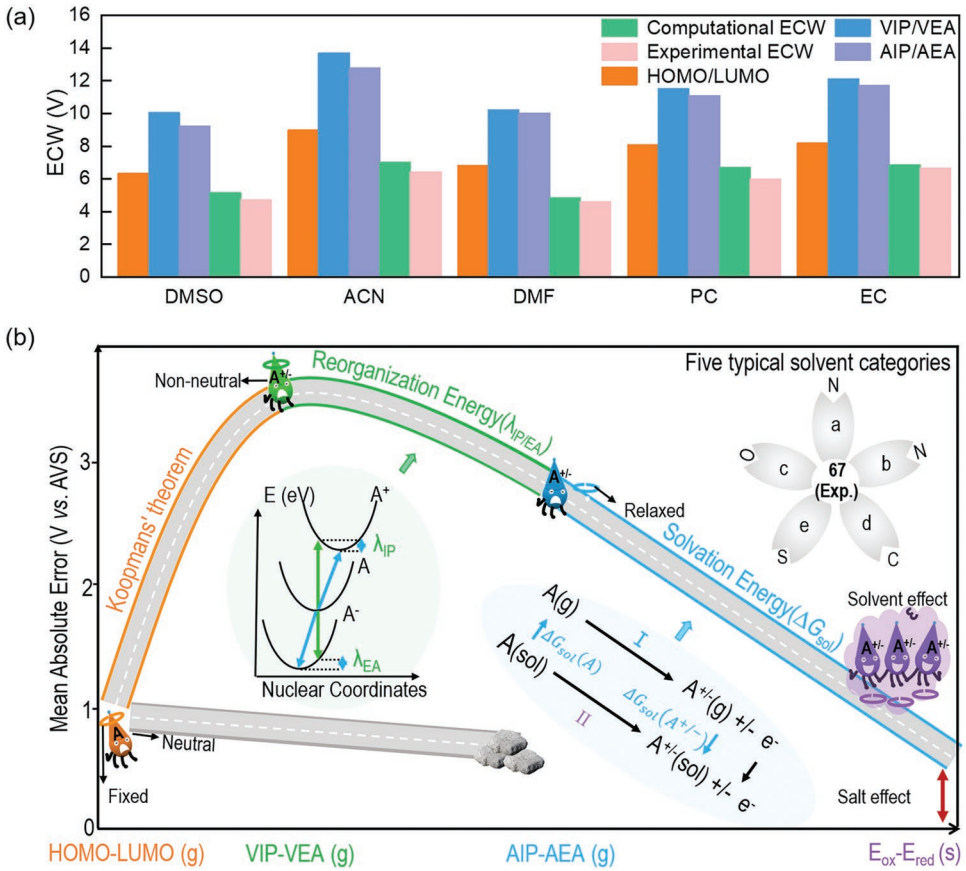

Figure 5. a) Differences in ECWs (in V) of 5 common solvents evaluated by HOMO/LUMO, VIP/VEA, b) AIP/AEA and thermodynamic cycle approach compared to their experimental values.

energy ($\lambda_{IP/EA}$ = VIP-AIP/AEA-VEA = $C_0 + C_1\Delta L + C_2\Delta D$) and solvation energy $\Delta G_{sol} = \Delta G_{sol}(A^{+/-}) - \Delta G_{sol}(A) = C_3 + C_4V$). Category a, b, c, d, and e represent amide-based, nitrile-based (CN), ether-based, carbonate-based (EC) and sulfone-based. I and II in thermodynamic cycle represent $\Delta G_g^{ox/red}(A) \approx$ AIP/-AEA-TΔS and $\Delta G_{sol}^{ox/red}(A)/E_{ox/red}$, respectively. Yellow, green, blue and purple cartoon balls represent HOMO/LUMO, VIP/VEA, AIP/AEA and thermodynamic cycle approach, respectively. The nooses on cartoon balls represent fixed/relaxation states of solvents. Neutral and non-neutral molecules are indicated by "(A)" and "($A^{+/-}$)", respectively. The purple shading represents the solvation effect, and we treat the solvent environment as a polarizable continuum medium characterized by a dielectric constant ε.

3.3. Screening wide ECW Solvents by the Proposed Thermodynamic Cycle Approach

Using the thermodynamic cycle proposed above, we next search for systems that have the potential to serve as wide ECW electrolytes for rechargeable batteries. A schematic illustration of the screening process used in this work is presented in **Figure 6**. As a first step, by traversing single functional-group substitutions of 211 electrolyte solvents extracted from above 141427 theoretical/experimental research papers, including above-mentioned 68 solvents with stable experimental ECWs, 16 solvents with experimental ECWs but irreversible structural changes during redox reactions, and 127 solvents with only theoretical ECWs, an original material database containing ECWs for 308 electrolyte solvents is established (Table S1, Supporting Information). In view of the complexity of multi-functional group substitutions as well as their generally high melting point properties (unlikely to be liquid at room temperature, as summarized in Table S6 (Supporting Information),[43] only single-functional group substitutions of above typical solvent categories are considered (Figure 6). Finally, combining above electrolytes with single-functional group substitution, a database containing 308 solvents is established (Table S1, Supporting Information).

From the redox potentials of 308 solvents shown in **Figure 7**a, the main distribution of potential is observed between 4.00 and 8.00 V versus Li^+/Li for oxidation and −0.50 and 1.00 V versus Li^+/Li for reduction.[44] Considering their high-voltage applications, we pay more attention to their oxidation potentials.[45] Based on this, by setting the oxidation potential value to be higher than 6.00 V versus Li^+/Li, 147 organic solvent candidates are selected, which contain commercial high oxidation potential electrolyte solvents, such as EC and DMC.[46] Notably, the calculated oxidation potentials of above solvents still differ from the experimental value by 0.68 V versus Li^+/Li (Table S1, Supporting Information). First, considering the dielectric constant of selected solvent phase Dimethyl sulfoxide (DMSO) is

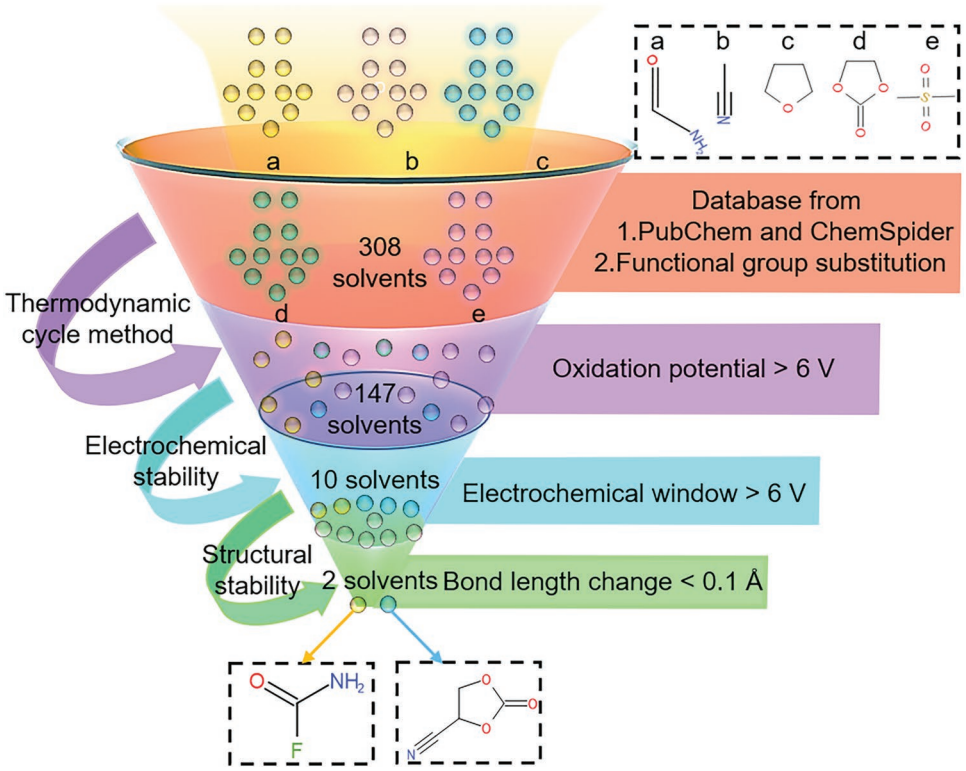

Figure 6. A screening funnel scheme is developed to select promising electrolyte solvents of rechargeable batteries. Categories a, b, c, d, and e indicate amide-based, nitrile-based (CN), ether (and acetals)-based, carbonate-based (EC) and else (e.g., boron ester-based, sulfone-based and phosphate-based) solvents, respectively. Substitutions are performed by traversing following functional groups in order of their electron donating abilities: $-N(CH_3)_2$, $-NH_2$, –OH, $-OCH_3$, $-CH_3$, $-C_6H_5$, –F, –Cl, –CHO, $-COCH_3$, $-COOCH_3$, –COOH, $-CF_3$, –CN and $-NO_2$. Finally, two omitted solvents, viz., Carbamic fluoride and 2-Oxo-1,3-dioxolane-4-carbonitrile with ECWs over 6 V and excellent structural stabilities are retrieved as promising solvents for rechargeable batteries. Here their chemical structures are also presented.

much higher than the critical value of 20, its influence on the accuracy of the calculation potential is excluded, as shown in Figure S11 (Supporting Information). Then, it is worth noting that the experimental values collected in this paper all on the working electrodes with minimal surface catalytic effects, such as Pt or glassy carbon, which also eliminates the inaccuracy of electrode potential calculation. Thus, this difference between calculated and experimental value is because only isolated solvents are considered, neglecting the influence of other factors in the experiments, such as the presence of additional electrolyte composition (solvents and/or ions), electrolyte concentration/PH and H-transfer reactions, as summarized in Table S7 (Supporting Information).[47] However, we emphasize that our screening results of solvents with high oxidation potentials are largely unaffected by this error, thus our calculated oxidation potentials can be used as an efficient criterion for pre-screening potentially wide ECW electrolyte systems.

By comprehensively considering the calculated thermodynamic cycle oxidation and reduction potentials of the selected 147 organic solvents, 10 candidates with wide ECWs (>6.00 V vs. Li^+/Li) that have not been reported experimentally are explored and considered as potential high-voltage battery electrolytes (Table S8, Supporting Information). Some important characteristics are observed: First, none of these 10 candidates contains amino ($-NH_2$) and methoxy ($-OCH_3$) electron-donating groups. This is due to the fact that although the addition of electron-donating groups reduces the reduction potentials, the reduction degree is generally much lower than that of oxidation potentials, resulting in a narrow ECW (Figure 7b; Table S1, Supporting Information). Thus, we infer that the introduction of electron-donating groups has an adverse effect on electrolyte ECW. Besides, although hydroxyl (-OH) and carboxyl (-COOH) substituted solvents well meet the wide ECW requirements, they are widely reported to undergo proton reduction at 2.00–4.00 V versus Li^+/Li,[48] making them generally not utilized as battery solvents. As a result, only 7 solvents are selected to be further considered as solvents for high voltage applications. Most importantly, all these 7 solvent candidates contain fluorine (-F) and cyano (-CN). This is reasonable because solvent with electron-withdrawing group enhances electrochemical stability to oxidation,[49] which is beneficial to achieve higher ECW (Figure 7c,d). This similar trend has also been verified by Yu et al.,[50] who evaluated the anodic stability of 1,2-diethoxyethane (DEE) and fluorinated-DEE by LSV, showing that fluorinated-DEE electrolytes, such as F3DEE with electron-withdrawing group $-CF_3$ (that is, ETFEE in our paper) exhibited higher oxidation potential (≈5.75 V vs. Li^+/Li) than DEE (≈4.5 V vs. Li^+/Li). Therefore, we conclude that the introduction of electron-withdrawing groups such as -F and -CN is a promising way for designing wide ECW electrolytes.

Finally, considering that solvents after electron transfer may exhibit significant structural changes, such as fragment

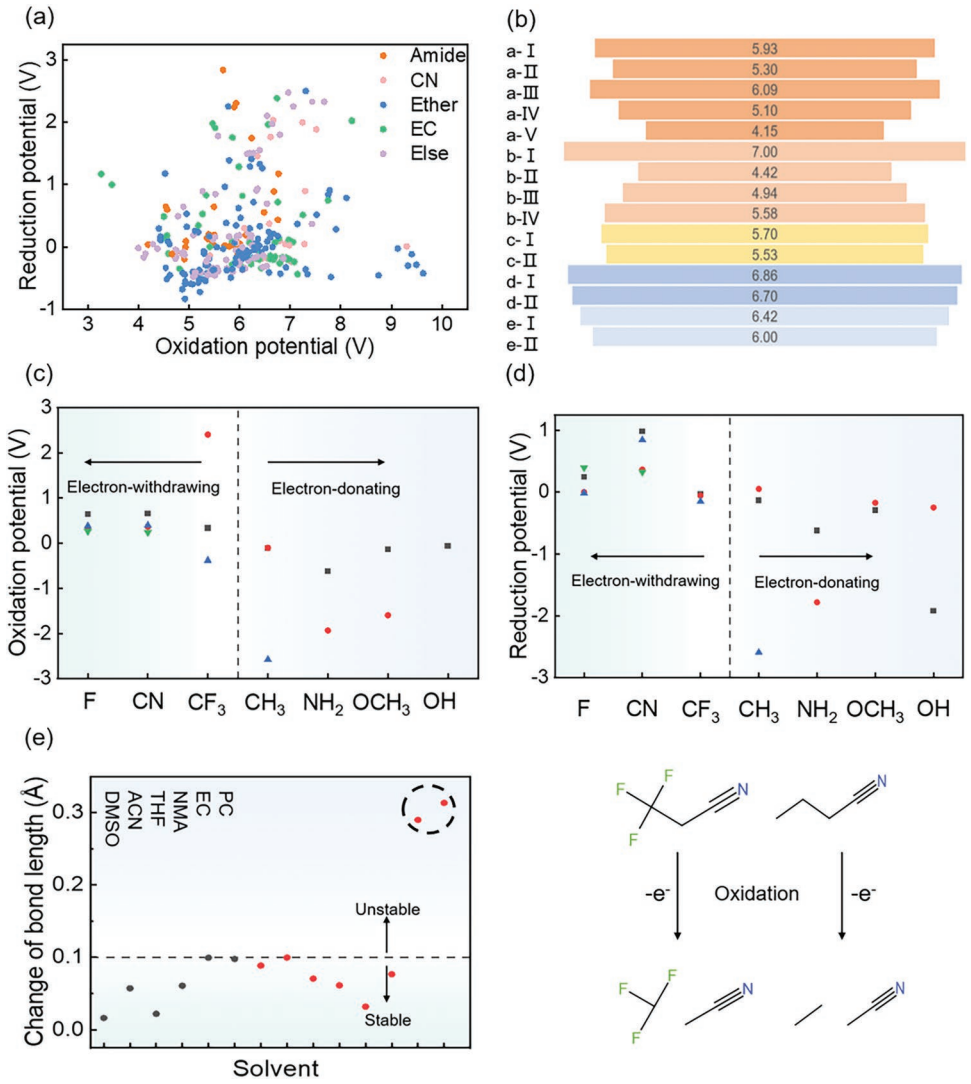

Figure 7. a) Distribution of oxidation potentials (in V vs. Li^+/Li) and reduction potentials (in V vs. Li^+/Li) for all 308 solvents. b) ECWs (in V) of basic molecules and substituted molecules by electron-donating functional groups. a-I–V: Formamide, Urea, Methoxyformamide, *N*-Methoxyformamide, Formylhydrazine; b-I–IV: ACN, Aminoacetonitrile, Benzylnitrile, Methoxypropionitrile; c-I–II: Tetrahydrofuran (THF), 2-Methyl tetrahydrofurane; d-I–II: EC, PC; e-I–II: Dimethyl sulfone , Ethyl methyl sulfone . Changes in c) oxidation potentials and d) reduction potentials (in V vs. Li^+/Li) between the basic molecules and substituted molecules. Functional groups to the left of black dashed line are electron-withdrawing, those to the right are electron-donating. e) Structural stability of 6 common solvents (from left to right are DMSO, ACN, THF, NMA, EC, and PC) vs. 7 selected solvents (from left to right are Carbamic fluoride, 2-Oxo-1,3-dioxolane-4-carbonitrile, Fluoroacetonitrile, Malononitrile, Methyl 2,2,2-trifluoroethyl carbonate, 3,3,3-Trifluoropropanenitrile, and Butanenitrile). The unstable 3,3,3-Trifluoropropanenitrile and Butanenitrile are highlighted in circle, both of which undergo fragment separation during single electron oxidation (right panel).

separation, which have a direct adverse effect on batteries performances due to the risk of decomposition,[19,49b] the structural stability of solvents should be further assessed. Here we use bond-length changes < 0.10 Å during redox process as a descriptor for screening potentially structurally stable species. The effectiveness of this simple geometric descriptor in finding stable organic solvents has been validated by successful reproduction of known materials.[19] As can be seen from Figure 7e, 2 (3,3,3-Trifluoropropanenitrile and Butanenitrile) of the seven screened solvents are excluded due to the bond breaking, and the remaining five are finally identified as the promising solvent candidates.

When we further examine the ECWs ranking of these five solvent candidates using traditional HOMO/LUMO method and our proposed new thermodynamic cycling approach, two characteristics are remarkable: First, the ranking of solvent ECWs predicted by the two methods is inconsistent, so that potential solvents with high ECWs (>6.00 V) screened by HOMO/LUMO cannot be verified by the new approach. For example, the ECW of Methanesulfonyl fluoride (FMS) calculated by HOMO/LUMO method is 8.67 V, but its actual thermodynamic cycle ECW is only 5.35 V (Table S1, Supporting Information), which is not included in the five solvent candidates screened above. Interestingly, although FMS has not been reported experimentally to provide a wide ECW, it has been mentioned in the theoretical literature as a high-voltage electrolyte for rechargeable batteries.[51] Besides, we return to the four

solvents reported in experiments and rank their ECWs using above methods as shown in Figure S12 (Supporting Information). It can be observed that compared with HOMO/LUMO method, the thermodynamic cycle approach not only reduces the ECW prediction MAE, but also provides consistency with the experiment in ECWs ranking, indicating its effectiveness in predicting ECWs.

Second and most importantly, the inaccuracy of traditional HOMO/LUMO method seriously leads to the neglect of potentially wide-ECW solvents. In this work, two solvent candidates, carbamic fluoride and 2-Oxo-1,3-dioxolane-4-carbonitrile, are omitted because their ECWs calculated by HOMO/LUMO method are only 8.15 and 7.80 V, respectively (Table S1, Supporting Information) which are less than the remaining solvent candidates (F-EMC: 8.60 V, Fluoroacetonitrile: 8.65 V, Malononitrile: 8.95 V, and FMS 8.66 V). However, their actual ECWs calculated by the thermodynamic cycle method are 6.32 and 6.40 V (Table S1 and Figure S13, Supporting Information), respectively, which are smaller than the remaining solvents (F-EMC: 6.78 V, Fluoroacetonitrile: 6.87 V, and Malononitrile: 6.91 V), but surprisingly larger than that of FMS (5.35 V), indicating their potential as rechargeable batteries electrolyte. In fact, F-EMC, Malononitrile and Fluoroacetonitrile also have been mentioned in theoretical literature to potentially exhibit excellent electrochemical stabilities similar to that of the familiar dinitrile solvents ($CN(CH_2)_nCN$) and fluorinated solvents (such as Fluoroethylene carbonate). For example, Amine et al.[52] found a theoretical ECW of up to 8.59 V for F-EMC by HOMO/LUMO method and the calculated oxidation potential is 7.01 V, which is in good agreement with our calculated value (7.02 V). Therefore, we screen two promising solvent candidates based on an examination incorporating ECWs and other experimental/theoretical physiochemical parameters, and expect that they will be experimentally verified in the near future.

Here, we also note that ECWs calculated by the HOMO/LUMO method for the above molecules are all 1 V larger than those calculated by the new thermodynamic cycling approach due to the inaccuracy of the HOMO/LUMO method, as shown in Figure 5a and Figures S13,S14 (Supporting Information). This again shows that in order to accurately calculate ECW, it is necessary to consider real redox conditions, such as geometrical relaxation and bulk solvent effects. In addition, we also find that both solvents are able to provide lower melting points or higher flash points than EC (Table S3, Supporting Information), indicating their potential to provide good cycle life and safety as solvents.[53] In conclusion, after further screening by structural stability and electrochemical stability, 2 previously omitted solvents (Carbamic fluoride and 2-Oxo-1,3-dioxolane-4-carbonitrile) are successfully retrieved as wide ECW solvents for rechargeable batteries.

4. Conclusions

In summary, the reasons of inaccuracy in ECW predictions by traditional methods (e.g., HOMO/LUMO) are explored via the collected 68 experimental data of solvents and the MAE of these methods is shown to reach up to 3.25 V versus absolute vacuum scale. Following this, we propose a high-accuracy thermodynamic cycle approach including two long-term overlooked corrections that can be identified as the keys dominating MAE, viz., reorganization-energy and solvation-energy, each of which can be quantified by two geometric descriptors (λ and ΔG_{sol}), ultimately reducing the prediction MAE to < 0.68 V (viz., with a 34.31% decrease in MAE compared to above HOMO/LUMO method). Subsequently, a database containing structural parameters, thermodynamic cycle ECWs and physicochemical properties of 308 common solvents is established. Moreover, 6 promising solvent candidates are suggested, 4 of which reproduced other calculated results evaluating them as excellent candidates for practical electrolytes (viz., Malononitrile: 6.91 V, Fluoroacetonitrile: 6.87 V, F-EMC: 6.78 V, FMS: 5.35 V), and the remaining candidates (Carbamic fluoride and 2-Oxo-1,3-dioxolane-4-carbonitrile) with ECWs over 6.00 V and excellent structural stabilities are waiting for validation.

It is worth noting that our proposed thermodynamic cycle-based intrinsic ECW model only considers the intrinsic redox stability of the solvent, while the realistic (i.e., non-intrinsic) stability of electrolyte includes the electrode interaction, since the redox of the electrolyte occurs through electron transfer at the interface with the solid electrode. Among them. the redox reaction at the electrode/electrolyte interface is highly dependent on the electrolyte compositions such as salt anion, solvent/additive, concentration and electrode surface activity state. Thus, future work still requires to focus on exploring above effects of redox potential between electrode materials and electrolyte, which not only can modify the prediction accuracy of the proposed approach, but also shed light on phenomena that cannot be explained by the non-intrinsic redox stability of solvent. For example, the theoretical calculation results show that the oxidation stability of EC is higher than that of DMC with or without the consideration of lithium ion. However, in the actual cycle of the battery, most of the electrolyte decomposition products come from EC.[24,54] In addition, electrolyte engineering requires not only wide ECW performance obtained by –F and –CN functional groups substitution, but also finely modulate molecular structure of electrolyte composition introducing partially fluorinated and locally polar $–CHF_2$ function group[50] or design non-fluorinated non-solvating cosolvent[34] to improve electrode stability, cycling performance and sufficient solvation for fast transport.

We also need to emphasize that the proposed thermodynamic cycle approach has strong applicability to predict the ECW of solvent molecular systems with weak interaction characteristics, but it still has limitation to solve the ECW prediction problem of systems with strong hydrogen bonds formed between solvent and solute molecules or ions with very high charge density. For example, when we calculate the ECW of water using the above proposed thermodynamic cycling approach, it is found to be 3.30 V instead of the experimentally measured 1.23 V.[3a,21] Therefore, the introduction of explicit solvation models is also highly desirable to solve more complex problems and proposed as a focus for the future research.

Supporting Information

Supporting Information is available from the Wiley Online Library or from the author.

Acknowledgements

This work was supported by the National Key Research and Development Program of China (No. 2021YFB3802104), the National Natural Science Foundation of China (Nos. U2030206, 11874254), the Shanghai Municipal Science and Technology Commission (No. 19DZ2252600), 21C Innovation Laboratory, Contemporary Amperex Technology Ltd. (No. 21C-OP-202205) and the Key Research Project of Zhejiang Laboratory (No. 2021PE0AC02).

Conflict of Interest

The authors declare no conflict of interest.

Data Availability Statement

The data that support the findings of this study are available in the supplementary material of this article.

Keywords

electrochemical window databases, electrolytes, reorganization energy corrections, solvation energy corrections, thermodynamic cycle approaches

Received: October 24, 2022
Revised: December 8, 2022
Published online: January 3, 2023

[1] a) Q. Zheng, Y. Yamada, R. Shang, S. Ko, Y.-Y. Lee, K. Kim, E. Nakamura, A. Yamada, *Nat. Energy* **2020**, *5*, 291; b) Y. G. Zou, Z. Cao, J. L. Zhang, W. Wahyudi, Y. Q. Wu, G. Liu, Q. Li, H. R. Cheng, D. Y. Zhang, G. T. Park, L. Cavallo, T. D. Anthopoulos, L. M. Wang, Y. K. Sun, J. Ming, *Adv. Mater.* **2021**, *33*, 2102964.
[2] a) X. Fan, C. Wang, *Chem. Soc. Rev.* **2021**, *50*, 10486; b) S. Zhang, J. Ma, Z. Hu, G. Cui, L. Chen, *Chem. Mater.* **2019**, *31*, 6033.
[3] a) P. Peljo, H. H. Girault, *Energ. Environ. Sci.* **2018**, *11*, 2306; b) C. Schütter, T. Husch, V. Viswanathan, S. Passerini, A. Balducci, M. Korth, *J. Power Sources* **2016**, *326*, 541.
[4] S. Kim, J. Chen, T. Cheng, A. Gindulyte, J. He, S. He, Q. Li, B. A. Shoemaker, P. A. Thiessen, B. Yu, L. Zaslavsky, J. Zhang, E. E. Bolton, *Nucleic. Acids. Res.* **2019**, *47*, D1102.
[5] H. E. Pence, A. Williams, *J. Chem. Edu.* **2010**, *87*, 1123.
[6] C. V. Amanchukwu, *Joule* **2020**, *4*, 281.
[7] a) J. Hwang, K. Matsumoto, R. Hagiwara, *Adv. Energy Mater.* **2020**, *10*, 2001880; b) Y. Zhang, C. Shi, J. F. Brennecke, E. J. Maginn, *J. Phys. Chem. B* **2014**, *118*, 6250.
[8] a) M. D. Scanlon, P. Peljo, M. A. Mendez, E. Smirnov, H. H. Girault, *Chem. Sci.* **2015**, *6*, 2705; b) D. H. Evans, *Chem. Rev.* **2008**, *108*, 2113.
[9] a) J. B. Goodenough, K.-S. Park, *J. Am. Chem. Soc.* **2013**, *135*, 1167; b) J. B. Goodenough, Y. Kim, *Chem. Mater.* **2010**, *22*, 587; c) D. Wang, Y. Jiao, W. Shi, B. Pu, F. Ning, J. Yi, Y. Ren, J. Yu, Y. Li, H. Wang, B. Li, Y. Li, C. Nan, L. Chen, S. Shi, *Prog. Mater. Sci.* **2023**, *133*, 101055.
[10] a) C. F. N. Marchiori, R. P. Carvalho, M. Ebadi, D. Brandell, C. M. Araujo, *Chem. Mater.* **2020**, *32*, 7237; b) H. Roohi, R. Salehi, *J. Electroanal. Chem.* **2020**, *877*, 114606.
[11] M. Korth, *Phys. Chem. Chem. Phys.* **2014**, *16*, 7919.
[12] a) S. P. Ong, O. Andreussi, Y. Wu, N. Marzari, G. Ceder, *Chem. Mater.* **2011**, *23*, 2979; b) E. R. Fadel, F. Faglioni, G. Samsonidze, N. Molinari, B. V. Merinov, W. A. GoddardIII, J. C. Grossman, J. P. Mailoa, B. Kozinsky, *Nat. Commun.* **2019**, *10*, 3360; c) X. Qu, Y. Zhang, N. N. Rajput, A. Jain, E. Maginn, K. A. Persson, *J. Phys. Chem. C* **2017**, *121*, 16126.
[13] a) J. B. Haskins, C. W. BauschlicherJr., J. W. Lawson, *J. Phys. Chem. B* **2015**, *119*, 14705; b) M. Isegawa, F. Neese, D. A. Pantazis, *J. Chem. Theory Comput.* **2016**, *12*, 2272.
[14] M. Frisch, G. Trucks, H. Schlegel, G. Scuseria, M. Robb, J. Cheeseman, G. Scalmani, V. Barone, B. Mennucci, G. Petersson, Gaussian, Inc., Wallingford CT **2009**.
[15] a) A. D. Becke, *Phys. Rev. A* **1988**, *38*, 3098; b) C. Lee, W. Yang, R. G. Parr, *Phys. Rev. B* **1988**, *37*, 785.
[16] W. J. Hehre, R. Ditchfield, J. A. Pople, *J. Chem. Phys.* **1972**, *56*, 2257.
[17] R. T. Boere, C. Bolli, M. Finze, A. Himmelspach, C. Knapp, T. L. Roemmele, *Chem.-Eur. J.* **2013**, *19*, 1784.
[18] C. P. Kelly, C. J. Cramer, D. G. Truhlar, *J. Phys. Chem. B* **2007**, *111*, 408.
[19] L. Cheng, R. S. Assary, X. Qu, A. Jain, S. P. Ong, N. N. Rajput, K. Persson, L. A. Curtiss, *J. Phys. Chem. Lett.* **2015**, *6*, 283.
[20] A. Lewis, J. A. Bumpus, D. G. Truhlar, C. J. Cramer, *J. Chem. Edu.* **2004**, *81*, 1265.
[21] O. Borodin, W. Behl, T. R. Jow, *J. Phys. Chem. C* **2013**, *117*, 8661.
[22] A. Wang, Z. Zou, D. Wang, Y. Liu, Y. Li, J. Wu, M. Avdeev, S. Shi, *Energy Storage Mater.* **2021**, *35*, 595.
[23] K. Xu, S. P. Ding, T. R. Jow, *J. Electrochem. Soc.* **1999**, *146*, 4172.
[24] K. Xu, *Chem. Rev.* **2004**, *104*, 4303.
[25] a) N. Heinrich, W. Koch, G. Frenking, *Chem. Phys. Lett.* **1986**, *124*, 20; b) G. Zhang, C. B. Musgrave, *J. Phys. Chem. A* **2007**, *111*, 1554.
[26] a) A. Boruah, M. P. Borpuzari, Y. Kawashima, K. Hirao, R. Kar, *J. Chem. Phys.* **2017**, *146*, 164102; b) J. Garza, J. A. Nichols, D. A. Dixon, *J. Chem. Phys.* **2000**, *113*, 6029; c) D. P. Chong, O. V. Gritsenko, E. J. Baerends, *J. Chem. Phys.* **2002**, *116*, 1760; d) T. Tsuneda, J. W. Song, S. Suzuki, K. Hirao, *J. Chem. Phys.* **2010**, *133*, 174101.
[27] I. N. Yakovkin, M. Gutowski, *Surf. Sci.* **2007**, *601*, 1481.
[28] a) M. V. Ivanov, D. Wang, D. Zhang, R. Rathore, S. A. Reid, *Phys. Chem. Chem. Phys.* **2018**, *20*, 25615; b) O. Borodin, *Curr. Opin. Electrochem.* **2019**, *13*, 86.
[29] J.-H. Pan, Y.-M. Chou, H.-L. Chiu, B.-C. Wang, *J. Phys. Org. Chem.* **2007**, *20*, 743.
[30] G. R. Hutchison, M. A. Ratner, T. J. Marks, *J. Am. Chem. Soc.* **2005**, *127*, 2339.
[31] H.-Y. Kim, *Restor. Dent. Electrochem. Endodont.* **2014**, *39*, 74.
[32] S. P. Ong, G. Ceder, *Electrochim. Acta* **2010**, *55*, 3804.
[33] A. V. Marenich, C. J. Cramer, D. G. Truhlar, *J. Phys. Chem. B* **2009**, *113*, 6378.
[34] J. Moon, D. O. Kim, L. Bekaert, M. Song, J. Chung, D. Lee, A. Hubin, J. Lim, *Nat. Commun.* **2022**, *13*, 4538.
[35] S. A. Martins, S. F. Sousa, *J. Comput. Chem.* **2013**, *34*, 1354.
[36] C. J. Cramer, D. G. Truhlar, *Accounts. Chem. Res.* **2008**, *41*, 760.
[37] B. Mennucci, J. Tomasi, R. Cammi, J. R. Cheeseman, M. J. Frisch, F. J. Devlin, S. Gabriel, P. J. Stephens, *J. Phys. Chem. A* **2002**, *106*, 6102.
[38] M. R. P. Long, C. M. Isborn, *J. Phys. Chem. B* **2017**, *121*, 10105.
[39] L. E. Roy, E. Jakubikova, M. G. Guthrie, E. R. Batista, *J. Phys. Chem. A* **2009**, *113*, 6745.
[40] K. C. Kim, T. Liu, S. W. Lee, S. S. Jang, *J. Am. Chem. Soc.* **2016**, *138*, 2374.
[41] S. C. Kim, X. Kong, R. A. Vila, W. Huang, Y. Chen, D. T. Boyle, Z. Yu, H. Wang, Z. Bao, J. Qin, Y. Cui, *J. Am. Chem. Soc.* **2021**, *143*, 10301.
[42] Y.-K. Han, J. Jung, S. Yu, H. Lee, *J. Power Sources* **2009**, *187*, 581.
[43] T. Husch, M. Korth, *Phys. Chem. Chem. Phys.* **2015**, *17*, 22596.
[44] M.-S. Park, Y.-S. Kang, D. Im, *ECS Trans.* **2015**, *68*, 75.
[45] M. S. Park, I. Park, Y. S. Kang, D. Im, S. G. Doo, *Phys. Chem. Chem. Phys.* **2016**, *18*, 26807.

[46] M. S. Park, Y. S. Kang, D. Im, S. G. Doo, H. Chang, *Phys. Chem. Chem. Phys.* **2014**, *16*, 22391.
[47] a) O. Borodin, M. Olguin, C. E. Spear, K. W. Leiter, J. Knap, *Nanotechnology* **2015**, *26*, 354003; b) C. H. Krause, P. Roering, H. Onishi, D. Diddens, J. H. Thienenkamp, G. Brunklaus, M. Winter, I. Cekic-Laskovic, *J. Power Sources* **2020**, *478*, 229047.
[48] A. J. Fry, *Synthetic organic electrochemistry*, John Wiley & Sons, **1989**.
[49] a) F. C. Krause, J.-P. Jones, M. C. Smart, K. B. Chin, E. J. Brandon, *Electrochim. Acta* **2021**, *374*, 137898; b) K. M. Pelzer, L. Cheng, L. A. Curtiss, *J. Phys. Chem. C* **2017**, *1*, 237.
[50] Z. Yu, P. E. Rudnicki, Z. Zhang, Z. Huang, H. Celik, S. T. Oyakhire, Y. Chen, X. Kong, S. C. Kim, X. Xiao, H. Wang, Y. Zheng, G. A. Kamat, M. S. Kim, S. F. Bent, J. Qin, Y. Cui, Z. Bao, *Nat. Energy* **2022**, *7*, 94.
[51] a) C.-C. Su, M. He, P. C. Redfern, L. A. Curtiss, I. A. Shkrob, Z. Zhang, *Energ. Environ. Sci.* **2017**, *10*, 900; b) N. Shao, X.-G. Sun, S. Dai, D.-e. Jiang, *J. Phys. Chem. B* **2012**, *116*, 3235.
[52] Z. Zhang, L. Hu, H. Wu, W. Weng, M. Koh, P. C. Redfern, L. A. Curtiss, K. Amine, *Energ. Environ. Sci.* **2013**, *6*, 1806.
[53] A. Balducci, *J. Power Sources* **2016**, *326*, 534.
[54] L. Xing, W. Li, C. Wang, F. Gu, M. Xu, C. Tan, J. Yi, *J. Phys. Chem. B* **2009**, *113*, 16596.